Catalysis Letters Vol. 100, Nos. 1–2, March 2005 (© 2005)
DOI: 10.1007/s10562-004-3091-z

Spinel $CuFe_2O_4$: a precursor for copper catalyst with high thermal stability and activity

Satoshi Kameoka[a,*], Toyokazu Tanabe[b] and An Pang Tsai[a,c]

[a]*Institute of Multidisciplinary Research for Advanced Materials, Tohoku University, 2-1-1 Katahira, Aoba-ku, Sendai, 980-8577 Japan*
[b]*Graduated School of Materials Science and Technology, Tokyo University of Science, 2641 Yamazaki, Noda, Chiba, 278-0022 Japan*
[c]*National Institute for Materials Science, 1-2-1 Sengen, Tsukuba, Ibaraki, 305-0047 Japan*

Received 9 July 2004; accepted 15 November 2004

Spinel $CuFe_2O_4$ has been studied as a precursor for copper catalyst. The spinel $CuFe_2O_4$ was effectively formed on the SiO_2 by calcination in air at 800 °C with the atomic ratio of Fe/Cu = 2. The spinel $CuFe_2O_4$ on the SiO_2 was reduced to fine dispersion of Cu and Fe_3O_4 particles by the H_2 reduction at 240 °C. After H_2 reduction at 600 °C, sintering of Cu particles over the $CuFe_2O_4/SiO_2$ (Fe/Cu = 2) was inhibited significantly, while fatal sintering of Cu particles over the Cu/SiO_2 (Fe/Cu = 0) occurred. The $CuFe_2O_4/SiO_2$ catalyst exhibited much higher activity and thermal stability for steam reforming of methanol (SRM), compared with the Cu/SiO_2 catalyst. The spinel $CuFe_2O_4$ on the SiO_2 can be regenerated after an intentional sintering treatment by calcination in air at 800 °C where the activity is also restored completely. Based on these findings, we propose that spinel $CuFe_2O_4$ is an effective precursor for a high performance copper catalyst in which the immiscible interaction between Cu and Fe (or Fe oxide) plays an important role in the stabilization of Cu particles.

KEY WORDS: $CuFe_2O_4$; spinel; immiscible; thermal stability; regeneration; methanol steam reforming.

1. Introduction

Copper-based catalysts are extensively studied due to their good catalytic performance in many reactions such as methanol synthesis and water gas shift reactions [1,2]. It is also well known that copper-based catalysts reveal high selectivity for steam reforming of methanol (SRM: $CH_3OH + H_2O \rightarrow 3H_2 + CO_2$), i.e. Cu catalysts are most promising for the SRM reaction [3–7]. However, difficulty of homogeneous dispersion of Cu particles on supports and poor thermal stability have been major drawbacks [3, 6]. To overcome these problems, several preparation methods for copper catalysts have been challenged [3–9]. Copper-containing spinel oxides possessing high performance in steam reforming of methanol [7], water gas shift reaction [8], CO oxidation [9] and removal of NO_x [10] have been reported. Matsukata *et al.* [7] reported that $CuAl_2O_4$ catalysts prepared by the coprecipitation method showed a high activity for steam reforming of methanol due to the formation of highly dispersed copper induced by reduction of $CuAl_2O_4$. Tanaka *et al.* [8] reported that Cu/MnO catalysts prepared via reduction of $CuMn_2O_4$ spinel oxide showed high activity in water gas shift reaction. In the previous literature, it has been commonly indicated that active sites responsible for reactions are copper species generated from Cu-containing spinel oxide (e.g., CuM_2O_4 type spinel). However, regeneration process of the copper species generated from the Cu-containing spinel oxide after the reduction and/or oxidation treatments have not been sufficiently investigated.

From the point of view of metallurgy, the interaction of second constituent metal (M) with copper involved in the CuM_2O_4 type spinel oxide seems to be a key factor for the formation and the catalytic redox process. However, little detailed work with respect to preparation of catalyst has been performed from this viewpoint. Recently, Tsai and Yoshimura [11] reported that an Al–Cu–Fe quasicrystal leached in NaOH aqueous solutions reveals excellent activity for steam reforming of methanol. Leaching leads to selective dissolution of Al, and consequently Cu and Fe segregate at the surface of quasicrystal. It was then claimed that the high catalytic activity was due to the immiscibility of Fe with Cu [11]. Actually, according to the Cu–Fe equilibrium phase diagram, Cu and Fe are neither form compounds nor mutually dissolve in the solid state [12]. Very recently, we have observed that calcination in air at 600 °C for the leaching Al–Cu–Fe quasicrystal furthermore improved the stability and activity [13]. We suppose that spinel $CuFe_2O_4$ might be important in this improvement. Therefore, we study catalytic activity of an oxide, spinel $CuFe_2O_4$, and the role of immiscibility between Cu and Fe in the oxide.

In this study, the catalytic behavior of spinel $CuFe_2O_4$ on an SiO_2 support for the SRM reaction has been examined. Validity of spinel $CuFe_2O_4$ used as a

---

*To whom correspondence should be addressed.
E-mail: kameoka@tagen.tohoku.ac.jp

1011-372X/05/0300–0089/0 © 2005 Springer Science+Business Media, Inc.

precursor compound for a high catalytic performance copper catalyst, i.e. high catalytic activity and thermal stability, is discussed.

2. Experimental

An SiO_2 support (Japan Aerosil Co. Ltd., SIO-50) had been precalcined in air at 900 °C (BET surface area: 50 m^2/g) to avoid structural change during the consequent high-temperature calcinations. Cu–Fe/SiO_2 catalysts were prepared by the impregnated method (incipient wetness) using $Cu(NO_3)_2$ (aq) and/or $Fe(NO_3)_3$ (aq) (atomic ratio of Fe/Cu = 0.5, 1, 2, 3; the weight loading of Cu was 10 wt%), and dried in air at 110 °C overnight. For comparison, 10 wt% Cu/SiO_2 (Fe/Cu = 0) and 10 wt% Fe/SiO_2 (Fe/Cu = ∞) were also prepared with the same method. All impregnated catalysts were calcined in air at 800 °C for 5 h. List of the samples is given in table 1.

The steam reforming of methanol (SRM) experiments were carried out in a conventional flow reactor at 100 kPa. Inlet partial pressure of methanol, water and nitrogen were 35.5, 52.7 and 13.2 kPa, respectively (LHSV of CH_3OH/H_2O mixture: 30 h^{-1}). Here nitrogen was used as dilutent. All the sample was pretreated at 240 °C with H_2 for 1 h in a flow reactor before SRM. The products were monitored by an on-line gas chromatograph [11]. The catalytic activity for the steam reforming of methanol was evaluated by the H_2 production rate (mL STP min^{-1} g-cat^{-1}). The data in the catalytic activity measurements were recorded when the reaction reached steady state after 30 min.

The phase identification of each sample was performed by X-ray diffraction (Rigaku RINT 2500) using Cu Kα (λ = 1.543 Å) radiation. The crystallite sizes of Cu were estimated from the XRD peak widths using the scherrer equation. The N_2O titration measurements were carried out with a conventional method as described previous report [14]. The H_2-TPR measurements were carried out using 50 mg of the catalyst from room temperature to 600 °C at a heating rate of 2 °C/min in a 30 mL/min flow of 5% H_2/Ar.

Table 1
List of each catalyst sample and initial crystalline phases

Catalyst Fe/Cu atomic ratio	Atomic fraction of Cu ($Cu_{atom}/(Cu_{atom} + Fe_{atom})$)	Observed crystalline[a] (phase)
0[b] (10 wt% Cu/SiO_2)	1	CuO
0.5[b]	0.67	CuO,($CuFe_2O_4$)
1[b]	0.50	CuO, $CuFe_2O_4$
2[b]	0.33	$CuFe_2O_4$
3[b]	0.25	$CuFe_2O_4$, Fe_2O_3
∞[c] (10 wt% Fe/SiO_2)	0	Fe_2O_3

[a] XRD measurement for the catalyst sample after air calcination at 800 °C for 5 h.
[b] Constant as 10 wt% Cu loading.
[c] 10 wt% Fe loading alone.

3. Results and discussion

Figure 1 shows the XRD patterns of Cu–Fe/SiO_2 catalysts with various Fe/Cu atomic ratio after calcination in air at 800 °C for 5 h. As shown in figure 1, the peaks responsible for spinel $CuFe_2O_4$ were observed for the Cu–Fe/SiO_2 catalysts (Fe/Cu = 0.5, 1, 2, 3) [15]. Additionally, the CuO was observed in the samples of Fe/Cu < 2, while the Fe_2O_3 was observed in the samples of Fe/Cu > 2. CuO and Fe_2O_3 were solely observed on Cu/SiO_2 (Fe/Cu = 0) and Fe/SiO_2 (Fe/Cu = ∞) catalyst, respectively. The list and the crystalline phases of each catalyst sample are summarized in table 1. From these results, it was found that the optimal value of the atomic ratio (Fe/Cu) for the formation of $CuFe_2O_4$ is consistent with the stoichiometry of the $CuFe_2O_4$ compound (Fe/Cu = 2). It should be noted that the spinel $CuFe_2O_4$ was formed from the mixture of CuO and Fe_2O_3 under high temperature, e.g., 700 °C [10,16].

Figure 2 shows the dependence of the fraction of Cu, i.e., $Cu_{atom}/(Cu_{atom} + Fe_{atom})$, on the rate of H_2 production in the steam reforming of methanol (SRM) over the different catalysts after H_2 reduction at 240 °C. For all Cu–Fe/SiO_2 catalyst, the rate of H_2 production increases with increasing reaction temperature (240–360 °C). As shown in figure 2, the rate of H_2 production varies with the fraction of Cu and it becomes clear at higher temperatures. Maxima of activity were observed around the stoichiometry of $CuFe_2O_4$ compound ($Cu_{atom}/(Cu_{atom} + Fe_{atom}) = 0.33$; Fe/Cu = 2), whereas the catalytic activities of the Cu/SiO_2 and the Fe/SiO_2 catalysts are very low even at 360 °C. This result indicates that the catalytic activity is significantly improved by coexistence of copper and iron, and the formation of $CuFe_2O_4$ compound is a key factor dominating catalytic activity.

Figure 3 shows the rate of H_2 production as a function of reaction temperature in the SRM over $CuFe_2O_4/SiO_2$ (Fe/Cu = 2) and Cu/SiO_2 catalysts after H_2 reduction at 600 °C. The activity of the $CuFe_2O_4/SiO_2$ catalyst decreased (process [I]) after H_2 reduction at 600 °C. The activity could not be detected even at 360 °C for the Cu/SiO_2 catalyst (figure 3(d)). Surprisingly, the activity could be recovered completely after the retreatment at 800 °C in air for the $CuFe_2O_4/SiO_2$ catalyst (process [II]) but entirely not for the Cu/SiO_2 catalyst. Obviously, the re-oxidation treatment brings about the reversible change in activity. The deactivation and the possible regeneration in the catalytic activities of the $CuFe_2O_4/SiO_2$ catalyst are correlated well with redox behaviors of the spinel $CuFe_2O_4$, which will describe below.

To understand the redox behavior of spinel $CuFe_2O_4$, we performed characterization on catalysts treated in

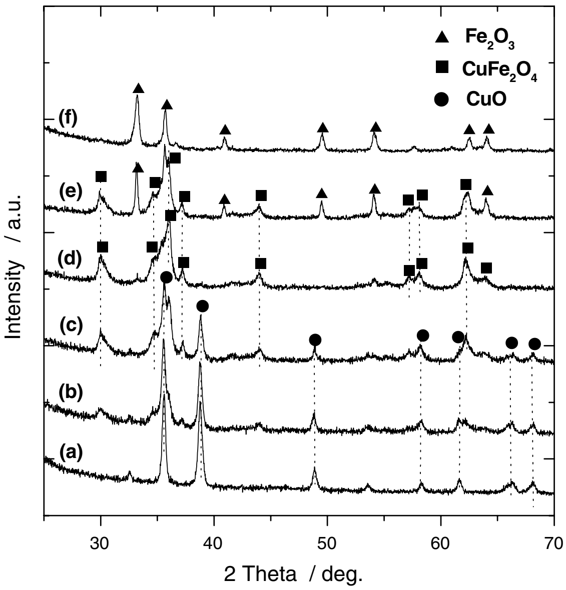

Figure 1. Powder X-ray diffraction patterns for Cu–Fe/SiO_2 catalysts with different Fe/Cu atomic ratio after air calcination at 800 °C for 5 h. (a) Fe/Cu = 0 (Fe = 0; Cu: 10 wt%), (b) Fe/Cu = 0.5, (c) Fe/Cu = 1, (d) Fe/Cu = 2, (e) Fe/Cu = 3 and (f) Fe/Cu = ∞ (Cu = 0; Fe: 10 w%).

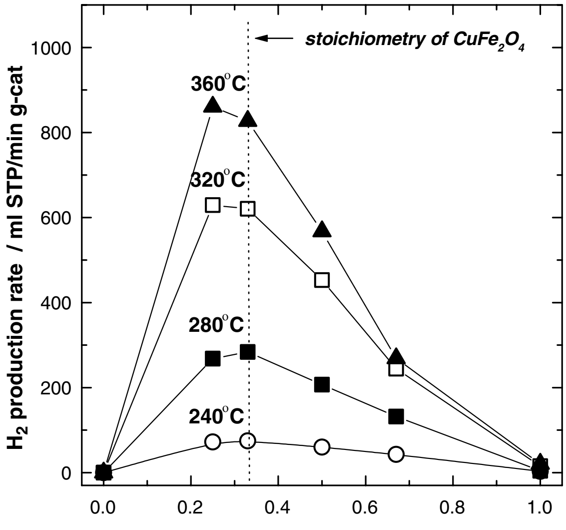

Figure 2. The rate of H_2 production versus fraction of Cu atom ($Cu_{atom}/(Cu_{atom} + Fe_{atom})$) in the steam reforming of methanol for catalysts given in figure 1. Reaction at (○) 240 °C, (■) 280 °C, (□) 320 °C and (▲) 360 °C.

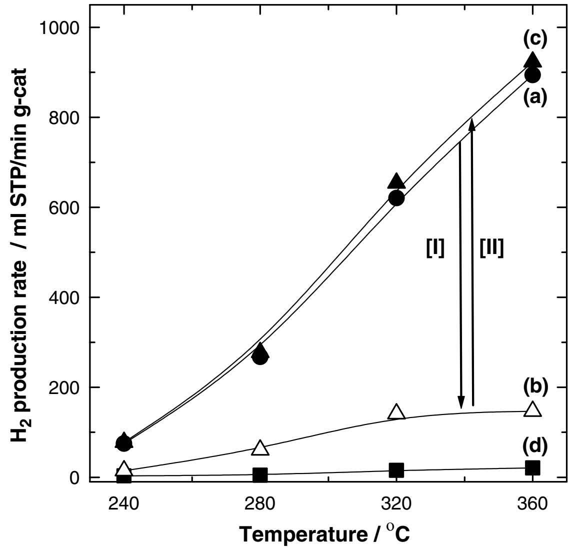

Figure 3. The rate of H_2 production versus reaction temperatures in the steam reforming of methanol for the $CuFe_2O_4/SiO_2$ (Fe/Cu = 2) catalyst. (●: a) air calcinations at 800 °C followed by H_2 reduction at 240 °C, (△: b) (a) followed by H_2 reduction at 600 °C, (▲: c) (b) followed by air recalcinations at 800 °C for 1 h and (■: d) Cu/SiO_2 catalyst after air calcinations at 800 °C for 5 h followed by H_2 reduction at 600 °C.

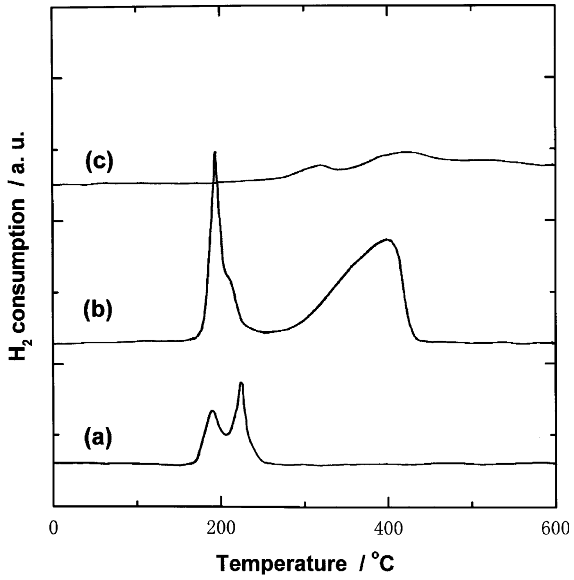

Figure 4. H_2-TPR profiles of the different catalysts after air calcinations at 800 °C. (a) Cu/SiO_2 (Fe/Cu = 0), (b) $CuFe_2O_4/SiO_2$ (Fe/Cu = 2) and (c) Fe/SiO_2 (Fe/Cu = ∞); TPR conditions: heating rate 2 °C/min in 5% H_2/Ar.

each process. Figure 4 shows the H_2-TPR profiles of Cu/SiO_2, $CuFe_2O_4/SiO_2$ (Fe/Cu = 2) and Fe/SiO_2 catalysts after calcination in air at 800 °C. Additionally, figure 5 shows the XRD patterns of Cu/SiO_2 and $CuFe_2O_4/SiO_2$ (Fe/Cu = 2) catalyst after air calcination at 800 °C followed by H_2 reduction at 240, 360 and 600 °C. As shown in figure 4(a), two reduction peaks around 190 and 220 °C observed for the Cu/SiO_2 catalyst, which are attributed to the reduction of dispersed copper oxide species and the bulk CuO, respectively [16, 17]. Total amount of H_2 consumed (H_2/Cu ratio) was 0.994, which is corresponding to the reduction of CuO to Cu (i.e., $CuO + H_2 \rightarrow Cu + H_2O$). Results of physical measurements of Cu/SiO_2 catalyst are given in table 2. As shown in figure 5 (f, g), only sharp diffraction peaks from Cu were observed after H_2

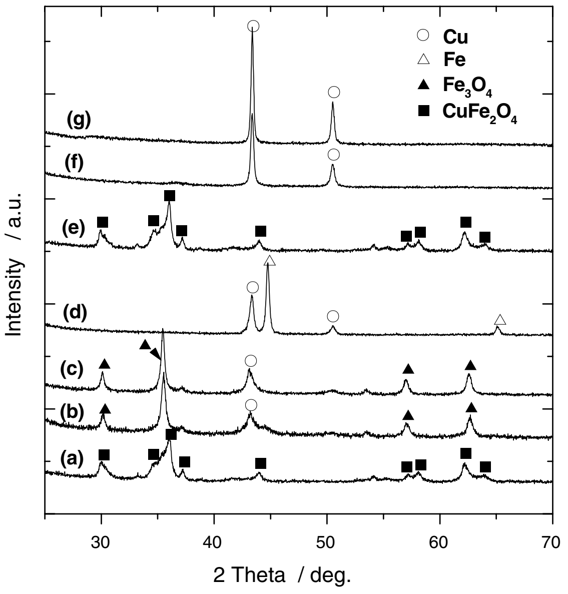

Figure 5. Powder X-ray diffraction patterns for $CuFe_2O_4/SiO_2$ catalyst (Fe/Cu = 2) and Cu/SiO_2 catalyst (Fe/Cu = 0). (a) $CuFe_2O_4/SiO_2$ catalyst after air calcination at 800 °C for 5 h, (b) (a) followed by H_2 reduction at 240 °C, (c) (a) followed by H_2 reduction at 360 °C, (d) (a) followed by H_2 reduction at 600 °C, (e) (d) followed by air calcinations at 800 °C for 1 h, (f) Cu/SiO_2 catalyst after air calcination at 800 °C followed by H_2 reduction at 360 °C and (g) (f) followed by H_2 reduction at 600 °C.

reduction at 360 and 600 °C, indicating that severe sintering of Cu particles readily occurs over the Cu/SiO_2 catalyst.

On the other hand, as shown in figure 4 (b), two pronounced reduction peaks were observed at 180–220 and 300–420 °C regions for the $CuFe_2O_4/SiO_2$ catalyst. Figures 5(a) and 5(b) show that the $CuFe_2O_4$ compound is reduced to Cu^0 and Fe_3O_4 particles below 240 °C. Subsequently, Fe_3O_4 particles is reduced to Fe^0 particles at higher temperatures (~600 °C: figure 5(d)). According to these results, it is clear that the reduction peak at lower temperature region in figure 4(b) is responsible for the reduction of $CuFe_2O_4$ species to Cu and Fe_3O_4 and that at higher temperature region in figure 4(b) is responsible for the reduction of Fe_3O_4 to Fe. The total amount of H_2 consumed (H_2/Cu ratio) was 3.90, which is consistent with that for the reduction of $CuFe_2O_4$ to Cu and Fe (*i.e.*, $CuFe_2O_4 + 4H_2 \rightarrow Cu + 2Fe + 4H_2O$). The changes in XRD patterns in a series of reduction treatments are unambiguously interpreted with the TPR profile for the $CuFe_2O_4/SiO_2$ catalyst. Results of N_2O titration and crystallite size of Cu particles estimated from XRD peaks are also summarized in table 2. Amount of O(a) species by N_2O titration for the $CuFe_2O_4/SiO_2$ is almost one order larger than that for the Cu/SiO_2. The crystallite size of copper particles for the $CuFe_2O_4/SiO_2$ catalyst even after the H_2 reduction at 600 °C is much smaller than that of copper particles over the Cu/SiO_2 catalyst. These results suggest that fine dispersion of Cu particles is performed by the reduction of $CuFe_2O_4$ in H_2 flow, and severe sintering of Cu particles is inhibited by the presence of iron even in the H_2 flow at high temperature (e.g., ~600 °C). Interestingly, as shown in figure 5(e), the spinel $CuFe_2O_4$ can be regenerated by treatment in air at 800 °C even after an intentional sintering of copper and iron particles. Consequently, the catalytic activity is restored to its original level (figure 3(c)).

For the Fe/SiO_2 catalyst, broad reduction peaks were observed above 280 °C (figure 4 (c)), which are attributed to the reduction from Fe_2O_3 to Fe_3O_4 and partially from Fe_3O_4 to Fe. Fe_3O_4 could not reduce to Fe completely during the H_2-TPR experiment (up to 600 °C). As shown in figures 4(b) and 4(c), the reduction temperature of iron oxides ($Fe_3O_4 \rightarrow Fe$) over $CuFe_2O_4/SiO_2$ shifted to lower temperatures, which indicates that reduction of iron oxides is promoted by the presence of copper. For this result, it is interpreted that the dissociative hydrogen atoms may migrate from the copper onto the iron oxides during H_2 treatment at high temperatures (i.e., spillover phenomenon [18]). Subsequently, iron oxides are reduced to iron by the reaction with H(a) atoms.

Recently, addition of iron to supported Cu catalysts such as Cu/SiO_2 and Cu/ZrO_2 causes a dramatic increase in activity and thermal stability against deactivation, which have been reported by several research groups [19, 20]. Chen *et al.* [19] reported that a small amount addition of Fe provided the advantages for copper catalysts both in promoting activity and in

Table 2
Results of the characterization of the Cu/SiO_2 and the $CuFe_2O_4/SiO_2$ catalyst

Catalyst[a] (Fe/Cu atomic ratio)	N_2O titration[b] (μmol/g-cat)	H_2-TPR[c]		Crystalline size of Cu[d]	
		LT (mmol/g-cat)	HT (mmol/g-cat)	360 (nm)	600 (nm)
Cu/SiO_2 (0)	41.6	1.56	–	29.7	52.8
$CuFe_2O_4/SiO_2$ (2)	387.8	1.95	4.17	7.9	18.5

[a] Constant as 10 wt% Cu loading (1.57 mmol Cu/g-cat).

[b] Total amount of N_2 produced by N_2O pulsed at rt after H_2reduction at 240 °C.

[c] Calculated from H_2-TPR profiles in the region of LT (< 240 °C) and HT (> 300 °C).

[d] Calculated from XRD patterns after H_2 reduction at 360 and 600°C using the Scherrer equation.

stabilizing catalyst dispersion. It was proposed that the iron species acts as a textural promoter to prevent copper sintering at high temperatures. Okamoto *et al.* [20] reported that the direct interaction between copper species and iron oxide clusters could form new species to inhibit sintering and enhance catalytic activity. However, the interaction between copper and iron in these catalyst systems is not sufficiently understood. In this study, we have shown a Cu catalyst with high thermal stability and revealing high catalytic activity where a spinel $CuFe_2O_4$ oxide acted as a precursor. The origin of high activity and high thermal stability is due to the formation of a composite structure induced by reduction of the $CuFe_2O_4$ where nano-scale Cu particles homogenously dispersed within Fe_3O_4 (i.e., fine dispersion of copper particles). Phase separation between copper and iron (or iron oxide) at nano-scale may be induced effectively because copper and iron in the spinel $CuFe_2O_4$ compound are regularly bonding through oxygen; *i.e.*, –O–Cu–O–Fe–O– [21]. Incorporating negligible solubility of oxygen in Cu and phase separation of Cu and Fe_3O_4 observed in figure 5(b), we may speculate that Cu is immiscible to Fe_3O_4. This is a key factor keeping high dispersion and high thermal stability of Cu particles. Moreover, as seen in the phase diagram of Cu–Fe binary system, Cu and Fe are immiscible [12], and when the $CuFe_2O_4$ fully reduced Cu and Fe particles maintain certain small size (~19 nm) as shown in table 2 and segregated on SiO_2. At this stage, although the activity decreases significantly, mixture with small grain size of Cu and Fe is favorable for the formation of $CuFe_2O_4$ at 800 °C in air. Through redox process, the phase transition from $CuFe_2O_4$ to Cu and Fe_3O_4, and to Cu and Fe and finally return to $CuFe_2O_4$, implying that $CuFe_2O_4$ is an ideal catalyst. Formation of spinel $CuFe_2O_4$ in which Cu and Fe are homogenous in atomic scale is the first key point. Immiscibility of Cu and Fe or Fe oxide is important in two ways; immiscibility of Cu and Fe_3O_4 sustains high dispersion of Cu particles and their stability, and that of Cu and Fe keeps Cu and Fe particles at certain small size which ensures quick regeneration of $CuFe_2O_4$ in air at 800 °C. By employing the similar concept, design of new catalyst is highly anticipated. Study in other CuM_2O_4 is in progress.

4. Conclusions

A Cu catalyst with fine dispersion of copper particles and high thermal stability can be prepared by the H_2 reduction at 240 °C for the spinel $CuFe_2O_4$ on the SiO_2 support. The catalytic activity of the $CuFe_2O_4/SiO_2$ catalyst for the steam reforming of methanol at high temperature (e.g., 360 °C) is much higher than those of the Cu/SiO_2 and the Fe/SiO_2 catalysts. These properties are ascribed to the reduction of the spinel $CuFe_2O_4$ and the subsequent immiscible interaction between Cu and Fe (or Fe oxide). Additionally, the spinel $CuFe_2O_4$ was readily regenerated by calcination in air at 800 °C even after the sintering of Cu by H_2 reduction at 600 °C. The present study demonstrates the validity of spinel $CuFe_2O_4$ as a precursor for a high catalytic performance copper catalyst.

References

[1] K. Klier, Adv. Catal. 31 (1980) 275.

[2] D.S. Newsome, Catal. Rev. Sci. Eng. 21 (1980) 275.

[3] N. Takezawa and N. Iwasa, Catal. Today 36 (1997) 45 and references therein.

[4] C.J. Jiang, D.L. Trimm, M.S. Wainwright and N.W. Cant, Appl. Catal. 93 (1993) 245.

[5] B.A. Peppley, J.C. Amphlett, L.M. Kearns and R.F. Mann, Appl. Catal. A 179 (1999) 21.

[6] T. Takeguchi, Y. Kani, M. Inoue and K. Eguchi, Catal. Lett. 83 (2002) 49.

[7] M. Matsukata, S. Uemiya and E. Kikuchi, Chem. Lett. (1988) 761.

[8] Y. Tanaka, T. Utaka, R. Kikuchi, T. Takeguchi, K. Sasaki and K. Eguchi, J. Catal. 215 (2003) 271.

[9] F. Severino, J.L. Brito, J. Laine, J.L.G. Fierro and A.L. Agudo, J. Catal. 177 (1998) 82.

[10] W.F. Shangguan, Y. Teraoka and S. Kagawa, Appl. Catal. B 8 (1996) 217.

[11] A.P. Tsai and M. Yoshimura, Appl. Catal. A 214 (2001) 237.

[12] T.B. Massalski (Editor-in-Chief), *Binary Alloy Phase Diagrams*, 2nd ed., Vol.2 (ASM International, USA, 1990), p. 1408.

[13] S. Kameoka, M. Terauchi and A.P. Tsai , to be published.

[14] J.W. Evans, M.S. Wainwright, A.J. Bridgewater and D.J. Young, Appl. Catal. 7 (1983) 75.

[15] X-ray powder diffraction data file, PDF#34–0425.

[16] L. Dong, Z. Liu, Y. Hu, B. Xu and Y. Chen, J. Chem. Soc., Faraday Trans. 94 (1998) 3033.

[17] W.-P. Dow, Y.-P. Wang and T.J. Huang, J. Catal. 160 (1996) 155.

[18] W.C. Conner Jr., G.M. Pajonk and S.J. Teichner, Adv. Catal. 34 (1986) 1.

[19] C.-S. Chen, W.-H. Cheng and S.-S. Lin, Appl. Catal. A 257 (2004) 97.

[20] Y. Okamoto, T. Kubota, H. Gotoh, Y. Ohto, H. Aritani T. Tanaka and S. Yoshida, J. Chem. Soc., Faraday Trans. 94 (1998) 3743.

[21] S. Krupicka and P. Novak, in: *Handbook on Ferromagnetic Materials*, E.P. Wohlfarth (ed.) Vol. 3 (North-Holland publishing Co., Amsterdam, 1982)..